



GLOBAL HEAT LOSS: NEW ESTIMATES USING DIGITAL GEOPHYSICAL MAPS AND GIS TECHNIQUES.

Fábio P. Vieira, Roberto R. Cardoso and Valiya M. Hamza, Observatório Nacional – ON/MCT, Rio de Janeiro

Copyright 2010, SBGf - Sociedade Brasileira de Geofísica

Este texto foi preparado para a apresentação no IV Simpósio Brasileiro de Geofísica, Brasília, 14 a 17 de novembro de 2010. Seu conteúdo foi revisado pelo Comitê Técnico do IV SimBGf, mas não necessariamente representa a opinião da SBGf ou de seus associados. É proibida a reprodução total ou parcial deste material para propósitos comerciais sem prévia autorização da SBGf.

Abstract

In the present work we report the progress obtained in estimating global conductive heat loss based on an updated heat flow data set and digital geophysical maps of tectonic provinces and age patterns. Modern GIS (Geographic Information Science) techniques were used in delimiting spatial domains of tectonic provinces and age patterns as sets of polygons and their intersections with areas of heat flow measurements. This procedure has allowed estimates of heat losses through area segments of intersecting “tectonic polygons” on a global scale. The main advantage of this method is that it minimizes the undesirable effects of data clustering.

The heat flow maps derived exclusively on the basis of tectonic characteristics and age provinces reveal patterns that are quite similar to those derived from observational data. This result is of considerable value in the procedure used in deriving global heat flow maps where it is necessary to assign estimated values of heat flow for areas where experimental work has not been carried out.

Introduction

Measurement of heat flow in boreholes penetrating the near surface layers of the Earth provides valuable information on the internal thermal field and estimates of global heat loss. The problem however is that experimental data are available only for selected regions, there being large areas without any data at all. One of the ways of getting around this problem is to look for empirical relations between heat flow and geological characteristics of the surface layers. Hamza (1967) proposed the existence of a possible correlation between heat flow and geologic age. Following this pioneering work Polyak and Smirnov (1968) and Hamza and Verma (1969) pointed out the possibility of developing empirical relations between heat flow and tectonic age. In later works of Chapman and Pollack (1975) and Pollack et al (1993) this empirical relation was used in estimating heat flow values for areas for which experimental data were not available.

In the procedure adopted by Chapman and Pollack (1975) the heat flow estimates are made on the basis of geological features identifiable in 5 x 5 cells. In the work of Pollack et al (1993) the procedure for referencing geology was based on a system of 1 x 1 equal longitude cells. The procedure for selection of dominant geology in

each cell and estimation of number of cells was manual and hence prone to generation of potential errors. Also, in cells with more than one geologic unit this procedure could lead to heat flow values being associated with incorrect geology unit.

In the present work we point out that such difficulties can easily be overcome with the use of modern techniques in handling geospatial data sets. Techniques developed in Geographic Information Science (GIS) are particularly suitable for elaboration of digital geological and geophysical maps and in handling irregularly spaced data sets. Other major advantages of GIS techniques include matching heat flow measurements with geology polygons and estimating errors with appropriate weighting by area. In the following items we outline the methodology employed and present the results obtained.

Use of Digital Geophysical Maps and GIS Techniques

The method used in this work makes use of global maps of tectonic and age provinces (Mooney et al, 1998). The digitized versions of these maps, reproduced in Figures (1) and (2) respectively.

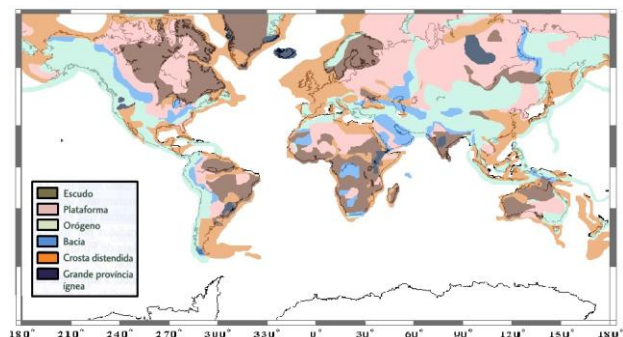


Figure -1. Digitized version of the map of Tectonic provinces.

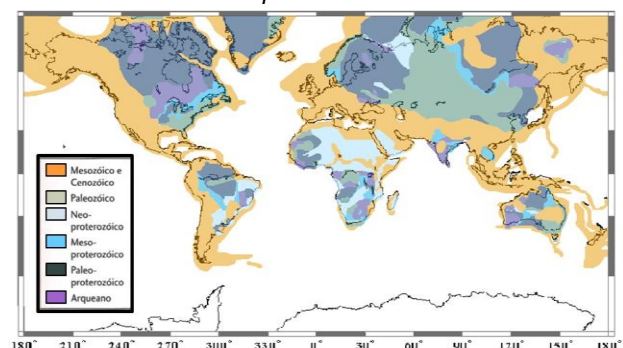


Figure -2. Digitized version of the map of Tectonic age.

GLOBAL HEAT LOSS: NEW ESTIMATES USING DIGITAL GEOPHYSICAL MAPS AND GIS TECHNIQUES.

Our starting point is a system of 1° x 1° degree equal longitude grid consisting of 64800 cells. Superposed on this grid system are a set of 190 polygons that delimit tectonic provinces and another set of 137 polygons that delimit the tectonic age pattern. Following this the area extents of these polygons were determined and values of mean heat loss calculated for the corresponding area segments. A brief summary of the system of polygons used in outlining tectonic provinces and age patterns is provided in Table (1).

Table (1) List of tectonic province and age polygons used in digital maps.

Location	Num. of Polygons to Tectonic Provinces		Num. of Polygons to Tectonic Age	
Africa	6	Platform	6	Archean
	9	Shields	4	Early Proterozoic
	1	Large Igneous Province	3	Middle Proterozoic
	6	Basin	6	Late Proterozoic
	3	Orogen	7	Paleozoic
	12	Extended Crust	5	Meso and Cenozoic
Asia	11	Platform	7	Archean
	6	Shields	6	Early Proterozoic
	2	Large Igneous Province	6	Middle Proterozoic
	9	Basin	3	Late Proterozoic
	10	Orogen	5	Paleozoic
	10	Extended Crust	6	Meso and Cenozoic
Europe	1	Platform	3	Archean
	2	Shields	2	Early Proterozoic
	1	Large Igneous Province	1	Middle Proterozoic
	0	Basin	0	Late Proterozoic
	4	Orogen	1	Paleozoic
	7	Extended Crust	3	Meso and Cenozoic
Greenland	0	Platform	0	Archean
	2	Shields	2	Early Proterozoic
	2	Large Igneous Province	0	Middle Proterozoic
	0	Basin	0	Late Proterozoic
	1	Orogen	1	Paleozoic
	2	Extended Crust	3	Meso and Cenozoic
North America	14	Platform	2	Archean
	3	Shields	4	Early Proterozoic
	2	Large Igneous Province	3	Middle Proterozoic
	4	Basin	0	Late Proterozoic
	7	Orogen	5	Paleozoic
	12	Extended Crust	7	Meso and Cenozoic
South America	3	Platform	2	Archean
	3	Shields	4	Early Proterozoic
	1	Large Igneous Province	2	Middle Proterozoic
	3	Basin	5	Late Proterozoic
	1	Orogen	1	Paleozoic
	5	Extended Crust	3	Meso and Cenozoic
Oceania	1	Platform	3	Archean
	3	Shields	3	Early Proterozoic
	0	Large Igneous Province	2	Middle Proterozoic
	1	Basin	2	Late Proterozoic
	8	Orogen	2	Paleozoic
	12	Extended Crust	7	Meso and Cenozoic
TOTAL	190		137	
TOTAL DE POLÍGONOS			327	

An illustrative example of the 1° x 1° cell system used in our work is provided in Figure (3) for the South American continent.

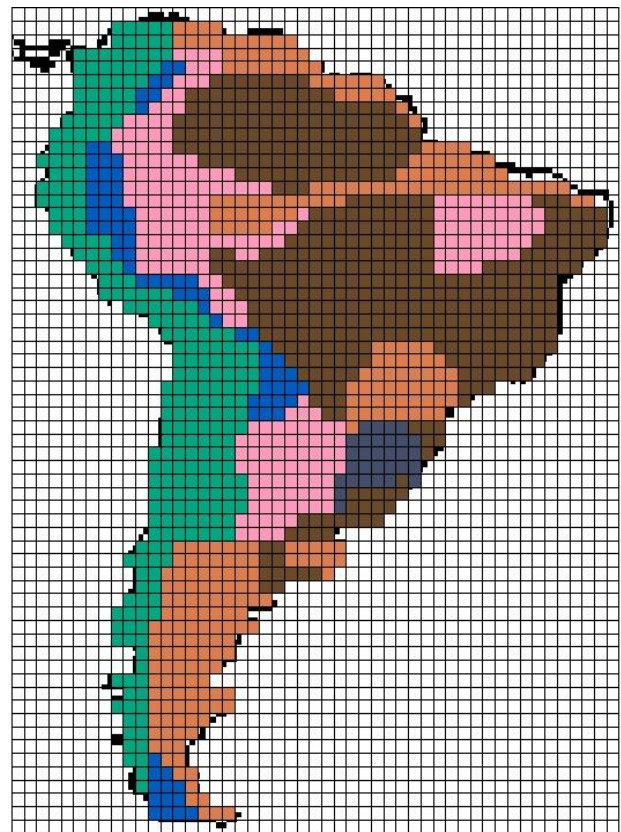


Figure (3) Example of the grid system used for the South American continent.

In calculating weighted mean values of heat flow for intersecting “tectonic polygons” we have assigned equal weights to both oceanic and continental data sets. This practice is based on the argument that regional scale hydrothermal circulation does not take place in stable oceanic crust. We consider that ocean bottom sediments act as blanketing cover over basement rocks and inhibits (rather than promotes) advective fluid flows. In fact the hypothesis of regional scale hydrothermal circulation in stable ocean crust (with down flow in areas of enhanced heat flux and up flow in areas of normal heat flux) contradicts the very basic principles of thermal convection.

Another outstanding feature of the present work concerns the use of heat flow data sets for ocean crust with ages less than 55 my. We have refrained from the practice (employed by some specific groups in the international geothermal community) of using theoretical heat flow values, derived from half-space cooling models, as substitutes for experimental data. The reason for the rejection is that half space cooling models account for conductive heat loss from stagnant fluid bodies and hence not representative of conditions in which lateral mass movements take place (which is the case mantle thermal convection).

The heat flow values assigned for age provinces are based on a modified version of the results reported by Hamza (1967), Polyak and Smirnov (1968) and Hamza and Verma (1969). The modifications introduced takes into consideration results of recent heat flow measurements in North America, Australia, Europe, South America, Africa and Asia. In addition, a constant

heat flow value of 45 mW/m² was assigned for the region of Antarctica. A summary of the heat flow values used are given in Table (2).

Table (2) Table with the average values of heat flow

Ages Tectonic	Geothermal flow						
	North America	Australia	Europe	South America	Africa	Asia	Antarctica
Cenozoic	75	80	78	81	81	63	-
Mesozoic	80	-	-	54	54	73	-
Paleozoic Shields	62	58	67	43	43	56	-
Proterozoic shields	55	73	38	34	34	45	45
Archean shields	41	43	-	32	32	36	-

Theoretical Heat Flow Maps

Estimation of heat flow values based on use of digital geophysical maps and age patterns have allowed derivation of theoretical heat flow maps. The results obtained for the system of 2° x 2° cells is illustrated in the global map of Figure (4). As expected theoretical heat flow values are in the range of 80 to 150mW/m² along the narrow belts of mid-ocean ridge systems and also in areas of young ocean crust. On the other hand the Proterozoic shield areas and cratonic nuclei in the interior parts of continental areas are characterized by relatively much lower theoretical heat flow (in the range of 20 to 60mW/m²). Intermediate values in the range of 60 to 80mW/m² are found for stable ocean basins, continental margins and areas of tectonic activity during Cenozoic, Mesozoic and Paleozoic.

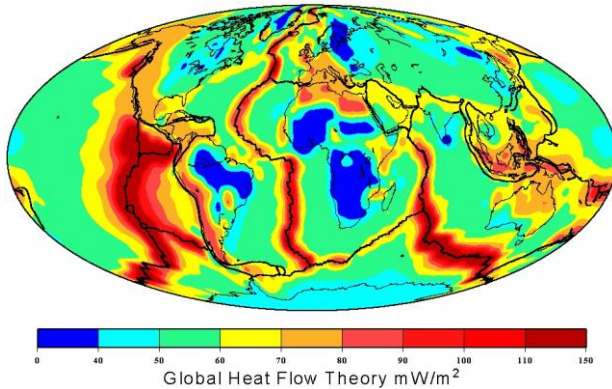


Figure (4) Theoretical Heat Flow Map derived from digital geophysical maps and empirical heat flow – age relation.

Distribution Observational Data

Availability of theoretical heat flow with appropriate weighting for the tectonic context have opened up the possibility of assigning improved values of heat flow for regions for which observational data are not currently available. Such theoretical values may be combined with the available observational heat flow data set in deriving new surface heat flow maps. In the present case we have used an updated data set (designated HCV10) of surface heat flow. The revised data set subsumes the IHFC data base (corrected for obvious errors in coordinate locations) and the data set reported in the recent study of Davies and Davies (2010). The total number of updated data is

over 40000. The distribution of the updated data set is illustrated in the map of Figure (5).

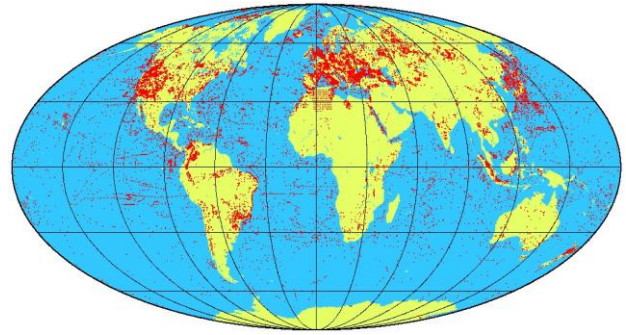


Figure (5) - Geographic distribution of updated observational heat flow data.

The data set illustrated in Figure (5) was appended with the set of theoretical heat flow values discussed earlier. The distributions of observational and theoretical data sets are illustrated in the 5° x 5° grid system map of Figure (6). In this figure the red color dots indicate cells with experimental data and the white color dots theoretical heat flow values.

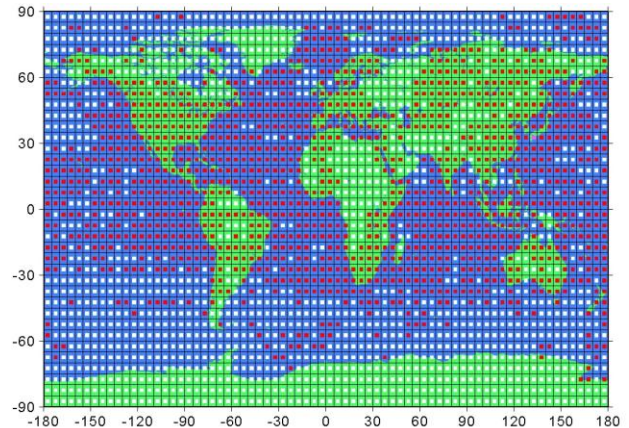


Figure (6) Map of grid system with cell size of 5° x 5°.

Discussion and Conclusions

The global surface heat flow derived on the basis of such a mixed data set is presented in Figure (6). It is readily apparent that the large scale features present in this map are quite similar to those of the theoretical heat flow map of Figure (4). Thus the divergent plate boundary regions (such as the Nazca plate in the Pacific, areas off the west coast of the United States, the Sea of Japan and the Red Sea) stands out as oceanic regions of relatively high heat flow (>80 mW/m²). Chains mid-ocean ridges in the Atlantic, Pacific and Indian oceans also appear as areas of high heat flow (typically in the range 90-150 mW/m²). The ocean basins and areas of low angle subduction appear to be characterized by normal heat flow (in the range 50-70 mW/m²). Moreover, the central parts of the mainland areas of Africa, Asia, North America, South America, Antarctica and Australia seem to be characterized by values of heat flow relatively low (<60 mW/m²).

Acknowledgments

This work was carried out as part of M.Sc. Thesis work of the first author. The second author is recipient of a research scholarship granted under the program PCI – Programa de Capacitação Institucional. We thank Dr. Iris Pereira Escobar for institutional support.

References

Cardoso, R.R., Ponte Neto, C.F. and Hamza, V.M., 2005, A reappraisal of global heat flow data. Proceedings, 9th International Congress of the Brazilian Geophysical Society, Salvador, Brazil, 6 pages.

Davies, J.H. and Davies, D.R., 2010, Earth's surface heat flux. *Solid Earth*, Vol. 1, p. 5-24.

Hamza, V.M., 1967, The relationship of heat flow with geologic age. Internal Report, National Geophysical Res. Institute, Hyderabad (India).

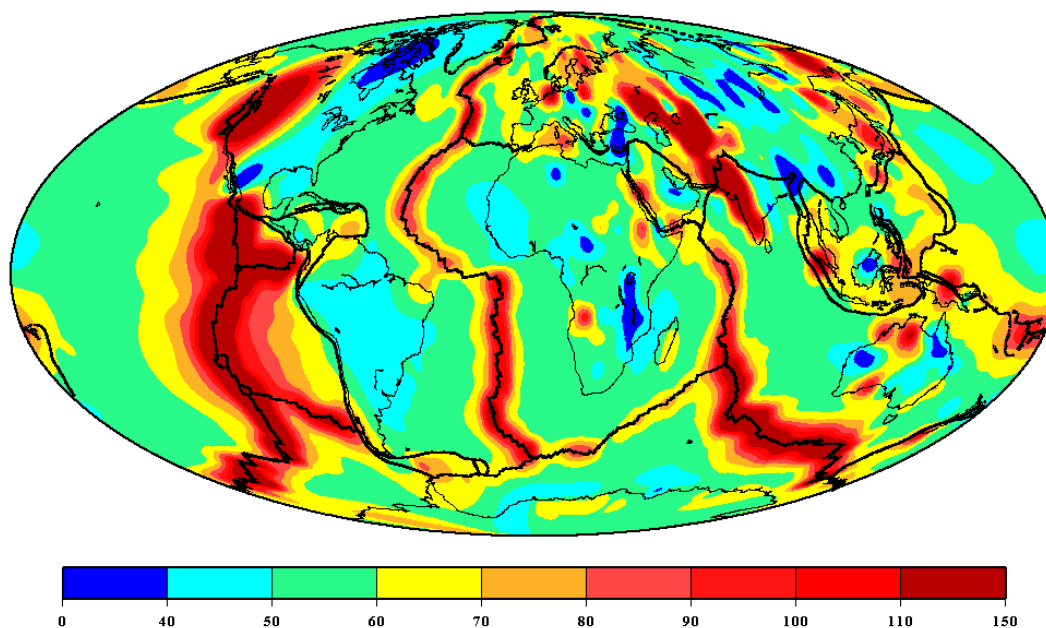
Hamza, V. M., Cardoso, R. R., and Alexandrino, C. H., 2008, A Magma Accretion Model for the Formation of Oceanic Lithosphere and Implications for Hydrothermal Circulation in Stable Ocean Crust and Global Heat Loss. *Int. J. Geophysics*, Vol. 2010, doi:10.1155/2010/146496, 16 pages.

Hamza, V.M., Cardoso, R.R. and Ponte Neto, C.F., 2008, Spherical Harmonic Analysis of Earth's Conductive Heat Flow". *International Journal of Earth Sciences*, 97:205-226.

Hamza, V.M., Cardoso, R.R. and Ponte Neto, C.F., 2008, Reply to Comments by Henry N. Pollack and David S. Chapman on "Spherical Harmonic Analysis of Earth's Conductive Heat Flow". *International Journal of Earth Sciences*, 97:233-239.

Mooney, W.D., Laske, G. and Masters T.G., 1998, CRUST 5.1: A global crustal model at 5° × 5°. *J. Geophys. Res.*, V. 103, No. B1, 727–747, 1998'

Muller, R.D., Roest, W.R., Royer, J., Gahagan, L.M. and Sclater, J.G., 1997, Digital isochrons of the world's ocean floor. *J. Geophys. Res.*, 102, B2, 3211–3214.



Global Heat Flow mW/m^2
Figure (5) *Global Map of Heat Flow*